

# Electrokinetics of Dielectric Non-Newtonian Bio Fluids with Heat Transfer Through a Flexible Channel: Numerical Study

Kh.S. Mekheimer<sup>1</sup>, W.M. Hasona<sup>2</sup>, A.A. El-Shehkipy<sup>3</sup>, A.Z. Zaher<sup>4</sup>

<sup>1</sup>*Math. Dep., Faculty of Sci., Al-Azhar Uni., Nasr City, Egypt  
kh\_Mekheimer@azhar.edu.eg*

<sup>2</sup>*Math. Dep., Faculty of Sci., Zagazig Uni., Egypt*

<sup>3</sup>*Math. Dep., college of Sci., Imam Abdurrahman Bin Faisal Uni., P.O.Box 31451, Dammam, Saudi Arabia*

<sup>4</sup>*Eng. Math. Phys. Dep., Faculty of Engineering, - Shubra - Benha Uni., Egypt  
abdullah.zaher@feng.bu.edu.eg*

Received: 20 March 2017; revised: 06 November 2017; accepted: 08 November 2017; published online: 31 December 2017

**Abstract:** Throughout this paper we investigate the effect of a vertical alternative current AC and heat transfer on the peristaltic flow of a couple stress dielectric fluid (blood flow model) in a symmetric flexible sinusoidal wavy channel. In order to solve the system of coupled non-linear partial differential equations, a program designed by Mathematica software "parametric NDSolve package" is used, which pertains to describe the momentum, the energy, and the electric potential that is obtained from using a regular perturbation method with small amplitude ratio. The numerical formulas of the mean velocity, the mean temperature, and the mean electric field are computed and the phenomenon of reflux (the mean flow reversal) is discussed. Moreover, the physical parameters effects of the problem on these formulas are described and illustrated graphically. The results reveal that the mean time averaged velocity is accelerated in the presence of AC electric field and decelerated for the couple stress fluid model (a special case of non-Newtonian fluid). The mean time averaged temperature is high in the presence of an alternative current AC electric field. This results model imply that the physiological role of AC electric field enhances blood circulation and this might help to eliminate the metabolic waste products and endogenous pains producing.

**Key words:** peristaltic transport, dielectric fluid, heat transfer, electric field, couple stress fluid

## I. INTRODUCTION

Electro kinetics "Electro-Fluid-Dynamics (EFD) or Electro Hydrodynamics (EHD) " is the study of the dynamics of electrically charged fluids, i.e. the motions of ionized particles or molecules and their interactions with electric fields with the surrounding fluid. Electro Hydrodynamics EHD covers the following types of particle and fluid transport mechanisms: electrophoresis, electro kinesis, dielectrophoresis, electro-osmosis, and electrorotation. It appears in many applications such as enhancement of drying rates, drag reduction, plasma actuators and gas pumps. Electro Hydrodynamics EHD equations of motion can be classified to two groups: hydrodynamic equations and electric field equations. Theo-

retically, Electro Hydrodynamics EHD flow was investigated by Woodson and Melcher [1]. The problem of the onset of convective instability in a horizontal layer of a dielectric fluid under a simultaneous action of a vertical alternative current AC electric field and a vertical temperature gradient was examined by Takashima [2, 3]. Also, the effect of vertical alternative current AC electric field and heat transfer on peristaltic flow of a viscous incompressible dielectric liquid sheet in asymmetrical flexible channel has been investigated by El-sayed et al. [4].

The temperature is associated with the motion of molecules within a fluid, being directly related to the kinetic energy of the molecules, including vibrational and rotational motion. Heat transfer is the energy transferred between two

points at different temperatures. It is significant in several industrial and medical applications such as heat conduction in tissues, heat transfer due to perfusion of the arterial-venous blood through the pores of the tissue, metabolic heat generation, and external interactions such as electromagnetic radiation emitted from cell phones. Also, thermodynamic aspects of blood may become crucial in processes like oxygenation and hemodialysis when blood is drawn out of the body. Considering the needs of investigations in the peristaltic movement of physiological fluids, many authors [5]– [10] have studied peristaltic flow with heat transfer.

When the additives combine in the fluid, the forces which exist in the fluid object the forces of additives. This objection produces a couple force and hence a couple stress is induced in the fluid. This type of fluid is known as couple stress fluid. In further investigation, many authors assumed blood to be a suspension of spherical rigid particles (red cells), this suspension of spherical rigid particles will give rise to couple stresses in a fluid. Also, the couple stress model plays an important role in understanding some of the non-Newtonian flow properties of blood. The theory of couple stress fluids developed by Stokes [11] has many biomedical, industrial, and scientific applications.

Lately, a number of studies for a Newtonian and non-Newtonian fluids with peristalsis have been reported [12]– [18], also the combined effects of heat transfer and couple stress fluid (as a special case of non-Newtonian) on the peristaltic transport of viscous fluid in a channel have been discussed by Mekheimer and Abd elmaboud [19] and coworkers [20]– [25].

All the above investigation on peristaltic transport does not take into account the effect of the couple stress fluid (as a blood flow model) and heat transfer with alternative current AC electric field also from the behavior of the couple stress fluid as a blood model, it is interesting to discuss the effect of alternative current AC electric field on blood flow.

Owing to the above-mentioned studies, we have investigated the interaction between the Electro Hydrodynamics EHD and the couple stress fluid (as a blood flow model) with heat transfer in a sinusoidal wavy channel (Peristaltic flow) by considering a small wave number. The velocity characteristic, temperature distribution, pressure gradient, the critical pressure and electric potential function are obtained numerically by a program designed by Mathematica 10 software, including of parametric NDSolve package. A motivation of the present analysis is the hope that such a problem will be applicable in many clinical applications.

## II. MATHEMATICAL MODEL OF THE PROBLEM

We consider a symmetric two dimensional channel of uniform width  $2d$  filled with an incompressible dielectric couple stress fluid. We assume an infinite sinusoidal wave train traveling along the walls. The lower and the upper walls are maintained at constant temperatures  $\theta_{00}$  and  $\theta_{10}$ , respectively. In addition to the temperature gradient, a vertical A.C. electric field is also imposed across the channel. The lower wall is grounded and the upper wall is kept at the electric potential  $\varphi_{10}$  as shown in Figure 1, the wall equation can be defined as,

$$h'(x', t') = d + a \cos \frac{2\pi}{\lambda} (x' - \frac{\kappa}{d} t'), \quad (1)$$

where  $d$ ,  $a$ ,  $\lambda$ ,  $\frac{\kappa}{d}$  and  $t'$  are width, amplitude, wavelength, velocity of the wave and time. In absence of external forces the equations of continuity and momentum for the flow of an incompressible dielectric couple stress fluid are given in the following form [4],

$$\nabla \cdot \vec{q} = 0, \quad (2)$$

$$\rho \left( \frac{\partial \vec{q}}{\partial t} + (\vec{q} \cdot \nabla) \vec{q} \right) = -\nabla p^* + \mu \nabla^2 \vec{q} - \gamma_c \nabla^4 \vec{q} + \vec{f}_e, \quad (3)$$

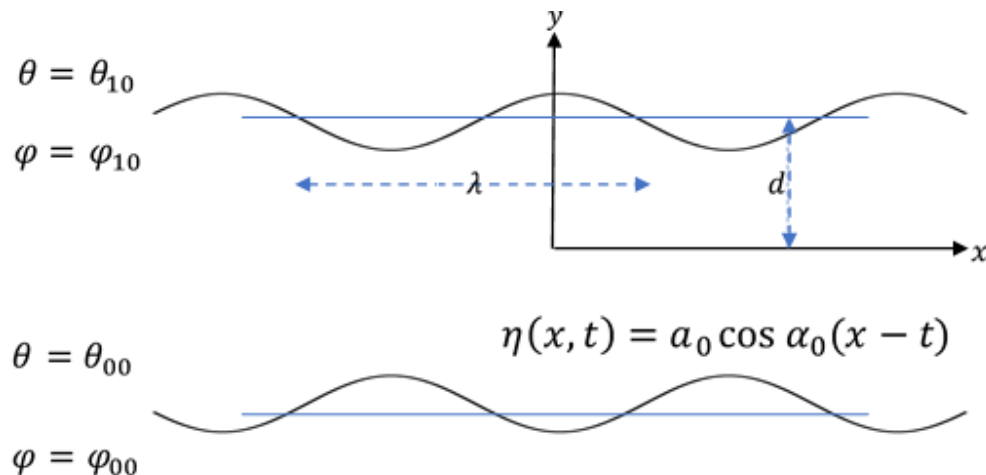


Fig. 1. Sketch of the physical model

$$\frac{\partial \theta'}{\partial t'} + \vec{q} \cdot \nabla \theta' = \kappa \nabla^2 \theta' + \gamma_c (\nabla \vec{q} \cdot \nabla \vec{q}) + \phi, \quad (4)$$

$$\vec{f}_e = \rho_e \vec{E} - \frac{1}{2} E^2 \nabla \varepsilon + \frac{1}{2} \nabla (\rho \frac{\partial \varepsilon}{\partial \rho} E^2), \quad (5)$$

where  $\mu$ ,  $\vec{q}$ ,  $\rho$ ,  $p'^*$ ,  $\phi$ ,  $\theta$ ,  $\kappa = \frac{K}{\rho c}$ ,  $K$ ,  $c$ ,  $\vec{f}_e$ ,  $\rho_e$ ,  $\vec{E}$ ,  $\varepsilon$  and  $\gamma_c$  are apparent viscosity of the fluid, velocity vector of the fluid, density, pressure, dissipation function, temperature, thermometric conductivity, thermal conductivity, specific heat, body forces of electrical origin per unit volume, free charge density, electric field, dielectric constant and associated constant with the couple stress.

Since there is no free charge, the Maxwell's equation following [27] are,

$$\begin{aligned} \nabla \cdot (\varepsilon \vec{E}) &= 0, \\ \nabla \times \vec{E} &= 0 \text{ or } \vec{E} = -\nabla \varphi', \end{aligned} \quad (6)$$

where  $\varphi'$  is the electric potential and  $\varepsilon$  is the dielectric constant which is assumed to be a function of temperature as follows [3],

$$\varepsilon = \varepsilon_0 (1 - \epsilon (\theta' - \theta_{00})), \quad (7)$$

where  $\varepsilon_0$  is the permittivity at vacuum,  $\epsilon$  is the thermal expansion coefficient of dielectric constant.

### III. BASIC GOVERNING EQUATIONS

The governing equations for two dimensional motion of this model are:

$$\begin{aligned} \frac{\partial u'}{\partial t'} + u' \frac{\partial u'}{\partial x'} + v' \frac{\partial u'}{\partial y'} &= -\frac{1}{\rho} \frac{\partial p'}{\partial x'} + \nu \nabla^2 u' - \frac{\gamma_c}{\rho} \nabla^4 u' + \frac{\varepsilon_0 \epsilon}{2\rho} \left( \frac{\partial \varphi'}{\partial y'} \right)^2 \frac{\partial \theta'}{\partial x'}, \\ \frac{\partial v'}{\partial t'} + u' \frac{\partial v'}{\partial x'} + v' \frac{\partial v'}{\partial y'} &= -\frac{1}{\rho} \frac{\partial p'}{\partial y'} + \frac{\nu}{e} \nabla^2 v' - \frac{\gamma_c}{\rho} \nabla^4 v' + \frac{\varepsilon_0 \epsilon}{2\rho} \left( \frac{\partial \varphi'}{\partial y'} \right)^2 \frac{\partial \theta'}{\partial y'}, \\ \frac{\partial \theta'}{\partial t'} + u' \frac{\partial \theta'}{\partial x'} + v' \frac{\partial \theta'}{\partial y'} &= \kappa \nabla^2 \theta' + \frac{\nu}{\rho} \left( 2 \left( \frac{\partial u'}{\partial x'} \right)^2 + 2 \left( \frac{\partial v'}{\partial y'} \right)^2 + \left( \frac{\partial u'}{\partial y'} + \frac{\partial v'}{\partial x'} \right)^2 \right) \\ &+ \frac{\gamma_c}{\rho} \left( \left( \frac{\partial^2 v'}{\partial y'^2} + \frac{\partial^2 v'}{\partial x'^2} \right)^2 + \left( \frac{\partial^2 u'}{\partial y'^2} + \frac{\partial^2 u'}{\partial x'^2} \right)^2 \right), \end{aligned} \quad (8)$$

$$\frac{\partial}{\partial y'} \left[ (1 - \epsilon (\theta' - \theta_{00})) \frac{\partial \varphi'}{\partial y'} \right] = 0,$$

where  $u'$ ,  $v'$  are the velocity components of the vector  $q$  in  $x'$ ,  $y'$  directions, respectively, and  $p' = p'^* - \frac{1}{2} (\rho E^2 \frac{\partial \varepsilon}{\partial \rho})$ . We introduce the stream function  $u' = \frac{\partial \psi'}{\partial y'}$ ,  $v' = -\frac{\partial \psi'}{\partial x'}$ , then we find

$$\begin{aligned} \frac{\partial^2 \psi'}{\partial t' \partial y'} + \frac{\partial \psi'}{\partial y'} \frac{\partial^2 \psi'}{\partial x' \partial y'} - \frac{\partial \psi'}{\partial x'} \frac{\partial^2 \psi'}{\partial y'^2} &= -\frac{1}{\rho} \frac{\partial p'}{\partial x'} + \nu \nabla^2 \frac{\partial \psi'}{\partial y'} - \frac{\gamma_c}{\rho} \nabla^4 \frac{\partial \psi'}{\partial y'} + \frac{\varepsilon_0 \epsilon}{2\rho} \left( \frac{\partial \varphi'}{\partial y'} \right)^2 \frac{\partial \theta'}{\partial x'}, \\ -\frac{\partial^2 \psi'}{\partial t' \partial x'} - \frac{\partial \psi'}{\partial y'} \frac{\partial^2 \psi'}{\partial x'^2} + \frac{\partial \psi'}{\partial x'} \frac{\partial^2 \psi'}{\partial y' \partial x'} &= -\frac{1}{\rho} \frac{\partial p'}{\partial y'} - \frac{\nu}{e} \nabla^2 \frac{\partial \psi'}{\partial x'} + \frac{\gamma_c}{\rho} \nabla^4 \frac{\partial \psi'}{\partial x'} + \frac{\varepsilon_0 \epsilon}{2\rho} \left( \frac{\partial \varphi'}{\partial y'} \right)^2 \frac{\partial \theta'}{\partial y'}, \\ \frac{\partial \theta'}{\partial t'} + \frac{\partial \psi'}{\partial y'} \frac{\partial \theta'}{\partial x'} - \frac{\partial \psi'}{\partial x'} \frac{\partial \theta'}{\partial y'} &= \kappa \nabla^2 \theta' + \frac{\nu}{\rho} \left( 2 \left( \frac{\partial^2 \psi'}{\partial x' \partial y'} \right)^2 + 2 \left( \frac{\partial^2 \psi'}{\partial y' \partial x'} \right)^2 + \left( \frac{\partial^2 \psi'}{\partial y'^2} - \frac{\partial^2 \psi'}{\partial x'^2} \right)^2 \right) \\ &+ \frac{\gamma_c}{\rho} \left( \left( \frac{\partial^3 \psi'}{\partial y'^2 \partial x'} + \frac{\partial^3 \psi'}{\partial x'^3} \right)^2 + \left( \frac{\partial^3 \psi'}{\partial y'^3} + \frac{\partial^2 \psi'}{\partial x'^2 \partial y'} \right)^2 \right), \end{aligned} \quad (9)$$

$$\frac{\partial}{\partial y'} \left[ (1 - \epsilon (\theta' - \theta_{00})) \frac{\partial \varphi'}{\partial y} \right] = 0.$$

For further analysis, we use the following non-dimensional variables and parameters:

$$\begin{aligned} x &= \frac{x'}{d}, \quad y = \frac{y'}{d}, \quad u = \frac{u'd}{\kappa}, \quad v = \frac{v'd}{\kappa}, \quad \eta = \frac{\eta'}{d}, \quad p = \frac{d^2 p'}{\rho \kappa^2}, \\ t &= \frac{\kappa t'}{d^2}, \quad \psi = \frac{\psi'}{\kappa}, \quad \theta = \frac{\theta'}{\beta d}, \quad \varphi = \frac{\varphi'}{E_0 d}, \quad \gamma = \frac{L}{L_2 R_e}. \end{aligned} \quad (10)$$

Using the non-dimensional variables and parameters given above in Eq. (9), we find that the equations which govern the flow for a dielectric couple stress fluid in terms of the stream function,

$$\begin{aligned}
\frac{\partial^2 \psi}{\partial t \partial y} + \frac{\partial \psi}{\partial y} \frac{\partial^2 \psi}{\partial x \partial y} - \frac{\partial \psi}{\partial x} \frac{\partial^2 \psi}{\partial y^2} &= -\frac{\partial p}{\partial x} + \frac{1}{R_e} \nabla^2 \frac{\partial \psi}{\partial y} - \frac{S}{R_e} \nabla^4 \frac{\partial \psi}{\partial y} + \frac{\gamma}{2} \left( \frac{\partial \varphi}{\partial y} \right)^2 \frac{\partial \theta}{\partial x}, \\
-\frac{\partial^2 \psi}{\partial t \partial x} - \frac{\partial \psi}{\partial y} \frac{\partial^2 \psi}{\partial x^2} + \frac{\partial \psi}{\partial x} \frac{\partial^2 \psi}{\partial y \partial x} &= -\frac{\partial p}{\partial y} - \frac{1}{e R_e} \nabla^2 \frac{\partial \psi}{\partial x} + \frac{S}{R_e} \nabla^4 \frac{\partial \psi}{\partial x} + \frac{\gamma}{2} \left( \frac{\partial \varphi}{\partial y} \right)^2 \frac{\partial \theta}{\partial y}, \\
\frac{\partial \theta}{\partial t} + \frac{\partial \psi}{\partial y} \frac{\partial \theta}{\partial x} - \frac{\partial \psi}{\partial x} \frac{\partial \theta}{\partial y} &= \nabla^2 \theta + \frac{E_c}{R_e} \left( 4 \left( \frac{\partial^2 \psi}{\partial x \partial y} \right)^2 + \left( \frac{\partial^2 \psi}{\partial y^2} - \frac{\partial^2 \psi}{\partial x^2} \right)^2 \right) + \\
&\frac{E_c S}{R_e} \left( \left( \frac{\partial^3 \psi}{\partial y^2 \partial x} + \frac{\partial^3 \psi}{\partial x^3} \right)^2 + \left( \frac{\partial^3 \psi}{\partial y^3} + \frac{\partial^2 \psi}{\partial x^2 \partial y} \right)^2 \right), \\
\frac{\partial}{\partial y} [(1 - \epsilon(\theta - \theta_{00})) \frac{\partial \varphi}{\partial y}] &= 0,
\end{aligned} \tag{11}$$

where  $R_e = \frac{\kappa}{\nu} = \frac{cd}{\nu}$  is the Reynolds number,  $L = \frac{\epsilon_0 E_0^2 d^2 (\epsilon \beta d)^2}{\mu \kappa}$  is electrical Rayleigh number,  $L_2 = \epsilon \beta d$  is adverse temperature gradient,  $\beta = \frac{\theta_{00} - \theta_{10}}{2d}$ ,  $S^2 = \frac{\gamma c}{\rho d^2 \nu}$  is the couple stress parameter (as a special case of Non Newtonian fluid),  $E_c = \frac{\kappa/d^2}{c\beta d}$  is the Eckert number,  $a_0 = \frac{a}{d}$  is the amplitude ratio and  $\alpha_0 = \frac{2\pi d}{\lambda}$  is the wave number.

The corresponding dimensionless boundary conditions in the wave frame are

$$\begin{aligned}
\frac{\partial \psi}{\partial y} = 0, \quad \frac{\partial \psi}{\partial x} = -a_0 \alpha_0 \sin \alpha_0(x-t), \quad \frac{\partial^3 \psi}{\partial y^3} = 0, \\
\theta = \frac{\theta_{10}}{\beta d}, \quad \varphi = \frac{\varphi_{10}}{E_0 d} \quad \text{at } y = 1 + \eta, \\
\frac{\partial \psi}{\partial y} = 0, \quad \frac{\partial \psi}{\partial x} = a_0 \alpha_0 \sin \alpha_0(x-t), \quad \theta = \frac{\theta_{00}}{\beta d}, \\
\frac{\partial^3 \psi}{\partial y^3} = 0, \quad \varphi = \frac{\varphi_{00}}{E_0 d} \quad \text{at } y = -(1 + \eta),
\end{aligned} \tag{12}$$

where  $\eta = a_0 \sin \alpha_0(x-t)$ .

#### IV. METHODOLOGY OF THE PROBLEM

We assume that the dimensionless quantities  $\psi$ ,  $p$ ,  $\theta$  and  $\varphi$  can be expanded, respectively, in powers of the amplitude ratio  $a_0$  as follows [26]:

$$\begin{aligned}
\psi &= \psi_0 + a_0 \psi_1 + a_0^2 \psi_2, \\
\theta &= \theta_0 + a_0 \theta_1 + a_0^2 \theta_2, \\
p &= p_0 + a_0 p_1 + a_0^2 p_2, \\
\varphi &= \varphi_0 + a_0 \varphi_1 + a_0^2 \varphi_2, \\
\frac{\partial \psi}{\partial x} &= \frac{\partial \psi_0}{\partial x} + a_0 \frac{\partial \psi_1}{\partial x} + a_0^2 \frac{\partial \psi_2}{\partial x},
\end{aligned} \tag{13}$$

where  $\frac{\partial p}{\partial x}$  be the pressure gradient. Substituting (13) into (11) and (12) and collecting terms of equal powers of  $a_0$ , we obtain three sets of coupled non linear differential equations with their corresponding boundary conditions in  $\psi_0$ ,  $\psi_1$  and

$\psi_2$ . The zero order set of differential equations in  $\psi_0$  represents the steady state and the solution of this problem in the case of free pumping takes the form,

$$\begin{aligned}
u_0 = 0, \quad v_0 = 0, \\
\theta_0(y) = -y + \frac{\theta_{00} + \theta_{10}}{2\beta d} \\
\varphi_0(y) = -\frac{a_1}{L_2} \ln(h + L_2 y) \\
p_0^*(y) = \frac{\gamma a_1^2}{2L_2[h + L_2 y]} + b_0,
\end{aligned} \tag{14}$$

where  $a_1 = \frac{\varphi_{10} L_2}{E_0 d \ln(1+2L_2)}$  is the externally imposed electrical field,  $b_0$  is an arbitrary constant and  $h = 1 + L_2$ .

The first order set of differential equations in  $\psi_1$  with corresponding boundary conditions are

$$\begin{aligned}
\psi_1 &= \frac{1}{2} F_1(y) \exp[i\alpha_0(x-t)] + C.C., \\
\varphi_1 &= \frac{1}{2} E_1(y) \exp[i\alpha_0(x-t)] + C.C., \\
\theta_1 &= \frac{1}{2} T_1(y) \exp[i\alpha_0(x-t)] + C.C.,
\end{aligned} \tag{15}$$

where the C.C. denotes the complex conjugate.

Thus, we get the equations,

$$\begin{aligned}
-S \frac{d^6 F_1(y)}{dy^6} + (1 + 3S\alpha_0^2) \frac{d^4 F_1(y)}{dy^4} \\
+ (-2\alpha_0^2 + i\alpha_0 R_e - 3\alpha_0^4 S) \frac{d^2 F_1(y)}{dy^2} \\
+ (-i\alpha_0^3 R_e + \alpha_0^4 + S\alpha_0^6) F_1(y) \\
- \frac{iR_e \alpha_0 L_2 a_1^2 \gamma}{(h + L_2 y)^3} T_1(y) \\
- \frac{iR_e \alpha_0 a_1 \gamma}{(h + L_2 y)} \frac{dE_1(y)}{dy} = 0, \\
\frac{d^2 T_1(y)}{dy^2} + (i\alpha_0 - \alpha_0^2) T_1(y) - i\alpha F_1(y) = 0, \\
\frac{d}{dy} \left( (h + L_2 y) \frac{dE_1(y)}{dy} + \frac{a_1 L_2 T_1(y)}{(h + L_2 y)} \right) = 0.
\end{aligned} \tag{16}$$

With the boundary conditions

$$\begin{aligned}
 \frac{dF_1}{dy}(\pm 1) &= 0, \\
 F_1(\pm 1) &= \pm 1, \\
 \frac{d^3 F_1}{dy^3}(\pm 1) &= 0, \\
 T_1(\pm 1) &= \pm 1, \\
 E_1(-1) &= -a_1, \\
 E_1(1) &= \frac{a_1}{1 + 2L_2}.
 \end{aligned} \tag{17}$$

The second order set of differential equations in  $\psi_2$  with their corresponding boundary conditions are

$$\begin{aligned}
 \psi_2 &= \frac{1}{2} [F_{20}(y) + F_2(y) \exp [i\alpha_0(x - t)] + C.C.], \\
 \varphi_2 &= \frac{1}{2} [E_{20}(y) + E_2(y) \exp [i\alpha_0(x - t)] + C.C.], \\
 \varphi_2 &= \frac{1}{2} [T_{20}(y) + T_2(y) \exp [i\alpha_0(x - t)] + C.C.].
 \end{aligned} \tag{18}$$

Hence, the steady part differential equations for  $F_{20}$ ,  $T_{20}$  and  $E_{20}$  takes the form

$$\begin{aligned}
 -S \frac{d^5 F_{20}}{dy^5} + \frac{d^3 F_{20}}{dy^3} &= \frac{iR_e \alpha_0}{2} \left[ -F_1 \frac{d^2 F_1^*}{dy^2} + F_1^* \frac{d^2 F_1}{dy^2} + \frac{a_1 \gamma}{h + L_2 y} \left( T_1 \frac{dE_1^*}{dy} - T_1^* \frac{dE_1}{dy} \right) \right] \\
 &\quad + 2c_{20}, \\
 \frac{d^2 T_{20}}{dy^2} &= \frac{i\alpha_0}{2} \left( \frac{dF_1^*}{dy} T_1 - \frac{dF_1}{dy} T_1^* - \frac{dT_1^*}{dy} F_1 + \frac{dT_1}{dy} F_1^* \right) - \frac{E_c}{R_e} \left[ 4\alpha_0^2 \frac{dF_1}{dy} \frac{dF_1^*}{dy} + \frac{d^2 F_1}{dy^2} \frac{d^2 F_1^*}{dy^2} + \right. \\
 \alpha_0^4 F_1 F_1^* + \alpha_0^2 \left( F_1^* \frac{d^2 F_1}{dy^2} + F_1 \frac{d^2 F_1^*}{dy^2} \right) &\left. \right] - \frac{E_c S}{R_e} \left[ \alpha_0^4 \frac{dF_1}{dy} \frac{dF_1^*}{dy} + \alpha_0^2 \frac{d^2 F_1}{dy^2} \frac{d^2 F_1^*}{dy^2} + \frac{d^3 F_1}{dy^3} \frac{d^3 F_1^*}{dy^3} + \right. \\
 \alpha_0^6 F_1 F_1^* - \alpha_0^2 \left( \frac{d^3 F_1}{dy^3} \frac{dF_1^*}{dy} + \frac{d^3 F_1^*}{dy^3} \frac{dF_1}{dy} \right) &\left. \right] - \alpha_0^4 \left( F_1^* \frac{d^2 F_1}{dy^2} + F_1 \frac{d^2 F_1^*}{dy^2} \right), \\
 \frac{d}{dy} \left[ (h + L_2 y) \frac{dE_{20}}{dy} - \frac{L_2}{2} \left( \frac{dE_1}{dy} T_1^* + \frac{dE_1^*}{dy} T_1 \right) + \frac{a_1 L_2 T_{20}}{h + L_2 y} \right] &= 0,
 \end{aligned} \tag{19}$$

with boundary conditions

$$\begin{aligned}
 \frac{dF_{20}}{dy}(\pm 1) &= \mp \frac{1}{2} \left( \frac{d^2 F_1}{dy^2}(\pm 1) + \frac{d^2 F_1^*}{dy^2}(\pm 1) \right), \\
 \frac{d^3 F_{20}}{dy^3}(\pm 1) &= \mp \frac{1}{2} \left( \frac{d^4 F_1}{dy^4}(\pm 1) + \frac{d^4 F_1^*}{dy^4}(\pm 1) \right), \\
 T_{20}(\pm 1) &= \mp \frac{1}{2} \left( \frac{dT_1}{dy}(\pm 1) + \frac{dT_1^*}{dy}(\pm 1) \right), \\
 E_{20}(-1) &= -\frac{a_1 L_2}{2} + \frac{1}{2} \left( \frac{dE_1}{dy}(-1) + \frac{dE_1^*}{dy}(-1) \right), \\
 E_{20}(1) &= -\frac{a_1 L_2}{2(h + L_2)} - \frac{1}{2} \left( \frac{dE_1}{dy}(1) + \frac{dE_1^*}{dy}(1) \right).
 \end{aligned} \tag{20}$$

The program was designed by using Mathematica 10 software including the use of parametric ND solve package to simulate the numerical solutions of the system of the partial differential equations (16), (17), (19) and (20).

Thus, the mean time-averaged velocity, the mean time-averaged heat and the mean time-averaged electric potential are respectively calculated by using the following equations

$$\bar{u}(y) = \frac{1}{2\pi} \int_0^{2\pi} u(y, t) dt = u_0(y) + \frac{a_0^2}{2} F'_{20}(y), \tag{21}$$

$$\bar{\theta}(y) = \frac{1}{2\pi} \int_0^{2\pi} T(y, t) dt = \theta_0(y) + \frac{a_0^2}{2} T'_{20}(y), \tag{22}$$

$$\bar{\varphi}(y) = \frac{1}{2\pi} \int_0^{2\pi} \varphi(y, t) dt = \varphi_0(y) + \frac{a_0^2}{2} E'_{20}(y). \tag{23}$$

## V. VALIDATION OF RESULTS

We compare our numerical solution (using ParametricNDSolve) with the analytical results obtained by Fung [26]. We find that when the couple stress parameter tends to zero (Newtonian fluid) and the electrical Rayleigh number tends to zero (No electric field), our numerical results are those as obtained by Fung and Yih [26] see Tab. 1.

## VI. GRAPHICAL RESULTS AND DISCUSSION

The purpose of these numerical computations is to illustrate the influence of various governing physical parameters, such as couple stress parameter  $S$ , pressure gradient  $\frac{\partial p_2}{\partial x}$ , electric Rayleigh number  $L$ , electrical parameter  $a_1$ , Eckert number  $E_c$ , and Reynolds number  $R_e$  on the mean time-averaged velocity, temperature and electric potential.

This section is divided into three subsections. In the first subsection, the effects of the various parameters are discussed on the mean time-averaged velocity and the mean time-averaged temperature. In the second subsection, we discuss the effects of the various parameters on the mean time-averaged electric potential. Moreover, the critical pressure gradient for reflux is illustrated in the third subsection.

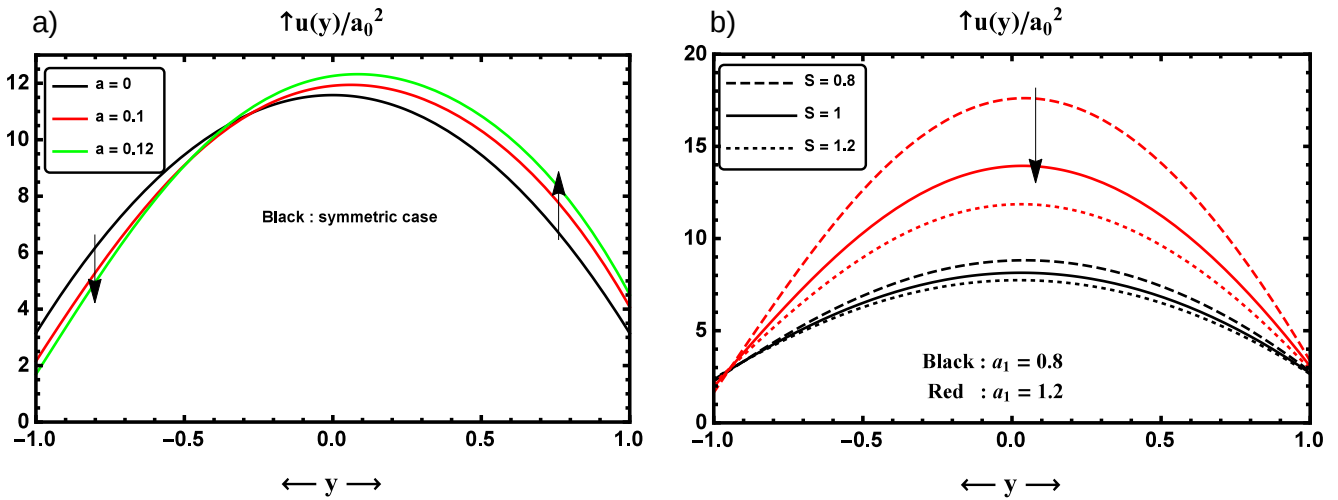


Fig. 2. Effect of the parameter  $a_1$  on the distribution of the mean velocity for  $Re = 5, L_2 = 0.5, \alpha_0 = 0.5, \frac{\partial p_2}{\partial x} = -1.7, L = 1000$  and (a) Newtonian fluid ( $S = 0$ ), (b)  $S \neq 0$ .

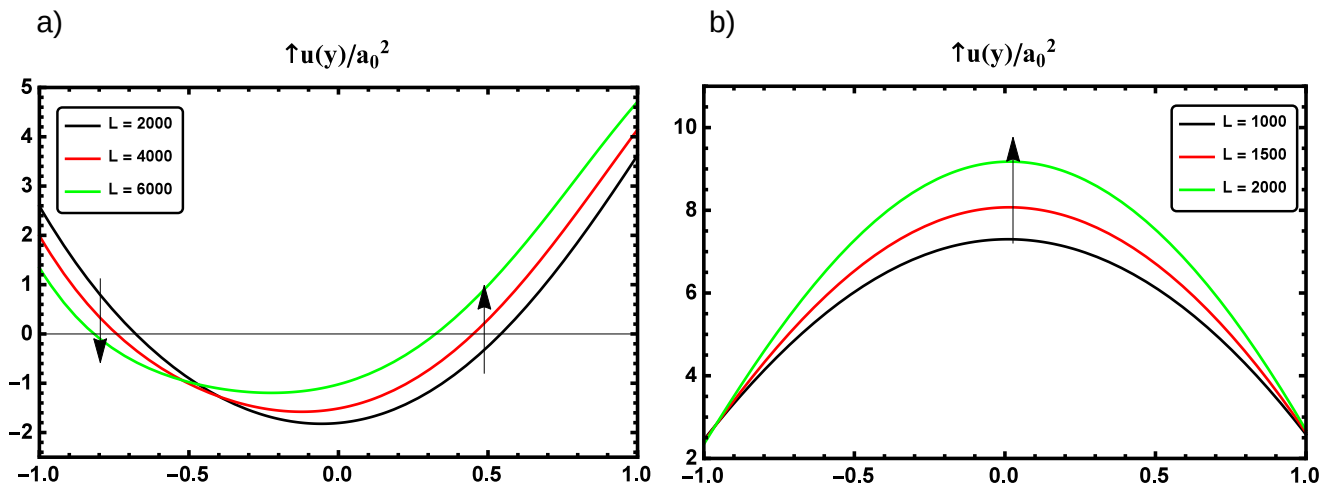


Fig. 3. Effect of the Raleigh parameter on the distribution of the mean velocity for  $R = 5, L_2 = 0.5, \alpha_0 = 0.5$  and (a) Newtonian fluid ( $S = 0$ ),  $a_1 = 0.1, \frac{\partial p_2}{\partial x} = 1$ . (b)  $S = 2, a_1 = 0.9, \frac{\partial p_2}{\partial x} = -1.7$

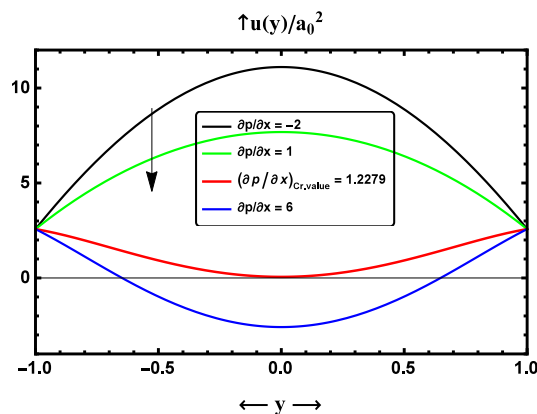


Fig. 4. Effect of the pressure gradient on the distribution of the mean velocity for  $L = 0, L_2 = 0.5, S = 0.2, Re = 10, a_1 = 0$ , and  $\alpha_0 = 0.5$

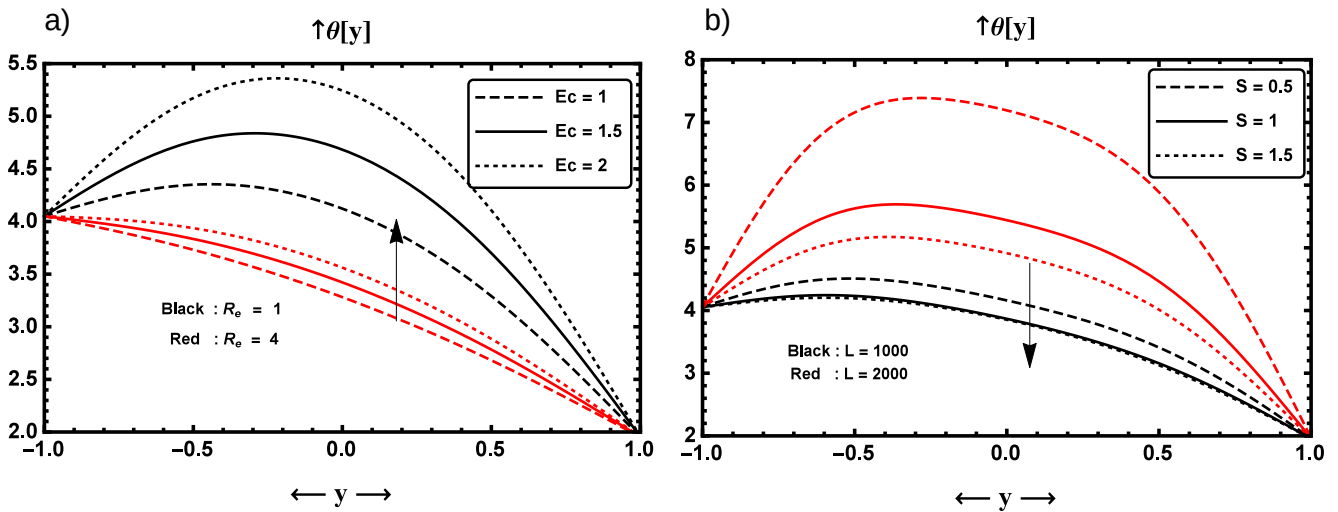


Fig. 5. Variation of the mean temperature vs  $y$  for  $L_2 = 0.5$ ,  $a_1 = 0.5$ ,  $a_0 = 0.3$ ,  $\frac{\partial p_2}{\partial x} = 10$ ,  $\alpha_0 = 0.5$  and (a) different values of Eckert number  $E_c$  and Reynolds number  $R_e$  for  $L = 2000$ ,  $S = 3$ . (b) different values of couple stress parameter  $S$  and Rayleigh number  $L$  for  $E_c = 1$ ,  $R_e = 1$

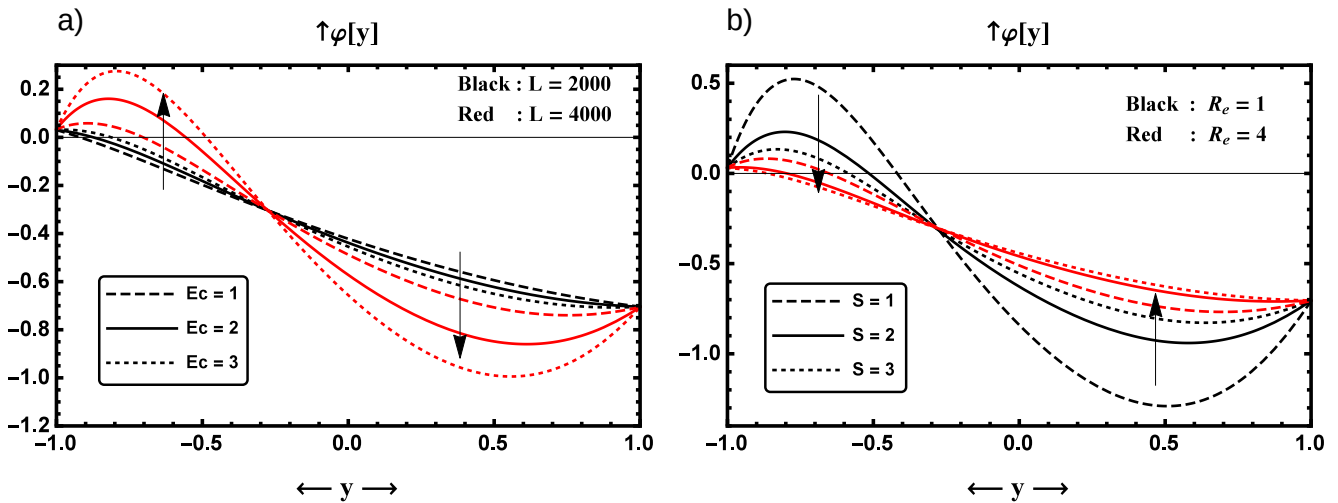


Fig. 6. Variation of the mean electric vs  $y$  for  $L_2 = 0.5$ ,  $a_1 = 0.5$ ,  $a_0 = 0.4$ ,  $\frac{\partial p_2}{\partial x} = 10$ ,  $\alpha_0 = 0.5$  and (a) different values of Eckert number  $E_c$  and Rayleigh number  $L$  for  $R_e = 5$ ,  $S = 0.2$ . (b) different values of couple stress parameter  $S$  and Reynolds number  $R_e$  for  $E_c = 1$ ,  $L = 4000$

Tab. 1. Comparison between analytical and numerical method on the mean time-averaged velocity  $\bar{u}(y)$   $R = 1$ ,  $\alpha_0 = 0.1$ .

| y    | $\bar{u}(y)$<br>Fung and Yih [26] | $\bar{u}(y)$<br>(Numerical solution)<br>at $S = 0$ and $L = 0$ | error     |
|------|-----------------------------------|--|-----------|
| -1.0 | 3.004063587                       | 3.004063594  | $10^{-7}$ |
| -0.8 | 3.364037470                       | 3.364037460  | $10^{-7}$ |
| -0.6 | 3.643999025                       | 3.643999016  | $10^{-7}$ |
| -0.4 | 3.843976610                       | 3.843976592  | $10^{-6}$ |
| -0.2 | 3.963970084                       | 3.963970063  | $10^{-7}$ |
| 0.0  | 4.003969599                       | 4.003969578  | $10^{-7}$ |
| 0.2  | 3.963970084                       | 3.963970065  | $10^{-7}$ |
| 0.4  | 3.843976610                       | 3.843976600  | $10^{-7}$ |
| 0.6  | 3.643999025                       | 3.643999021  | $10^{-7}$ |
| 0.8  | 3.364037470                       | 3.364037469  | $10^{-7}$ |
| 1.0  | 3.004063587                       | 3.004063590  | $10^{-7}$ |

## VI. 1. Mean velocity and temperature

Figs. 2–4 elucidate the variations of the mean velocity distribution  $u(y)$  with  $y$  for various values of the indicated parameters. Fig. 2 (a) reveals that in the absence of the electrical field and the couple stress parameter i.e. the electrical parameter  $a_1 = 0$  and the couple stress parameter  $S = 0$  (Non-Newtonian fluid), the behavior of the mean velocity  $u(y)$  is symmetric and becomes asymmetric for  $a_1 \neq 0$ , where the velocity increases towards the upper wall of the channel while decreases towards the lower one; this occurs according to the boundary conditions of the electric potential  $\varphi(y)$ . Interpretation physicist, the existence of the electric field decreases the density of the fluid which makes the fluid molecules freely moving, and this leads to an increase in the fluid velocity. In Fig. 2 (b), we observe that for the couple stress parameter  $S \neq 0$  (Newtonian fluid), the effect of the electric field parameter  $a_1 = 0$  makes a slight difference on the fluid velocity at the walls. In addition to this, the behavior of the mean velocity  $u(y)$  increases with the increase of the electrical parameter  $a_1$  but decreases with the increase of the couple stress parameter  $S$ , i.e. the increases of the electrical parameter accelerate the flow velocity. Fig. 3 (a,b) discusses the effect of the electric Rayleigh number  $L$  on the distribution of the mean velocity  $u(y)$ , where for the reversal flow case ( $\frac{\partial p_2}{\partial x} = 1$ , Newtonian fluid  $S = 0$ ), the reversal flow decreases as an electric Rayleigh number  $L$  increases for the region near to the upper wall ( $\varphi(y) \neq 0$ ) but a reverse effect occurs for the region near to the lower one ( $\varphi(y) = 0$ ), i.e. a reduction in the reversal flow occurs under the influence of the electric potential as shown in Fig. 3 (a). When the couple stress parameter  $S \neq 0$ , it is found that the effect of the electric Rayleigh number  $L$  on the mean velocity  $u(y)$  has a slight effect for a closer region near the walls. Also, we note that the mean velocity  $u(y)$  increases with a large value

of the electric Rayleigh number  $L$  as seen in Fig. 3 (b). Fig. 4 shows the variety of  $u(y)$  vs  $y$  for different values of the pressure gradient  $\frac{\partial p_2}{\partial x}$  and we can see that as  $\frac{\partial p_2}{\partial x}$  increases, a reflux flow (back flow) will be seen and it is important to note that the reflux occurs in the central region of the channel and when the pressure gradient attains a certain value (critical value,  $\frac{\partial p}{\partial x} \text{ cr. value} = 1.2279$ ) the fluid velocity at the channel center ( $y = 0$ ) will be zero.

Fig. 5 (a,b) are sketched to study the temperature distribution  $T(y)$  for different values of the problem parameters. Fig. 5 (a) is plotted to show the variation of the mean time-averaged temperature  $T(y)$  for different values of the Eckert number  $E_c$  and the Reynolds number  $Re$  while all other parameters are kept fixed. It is noticeable that the higher value of the Eckert number  $E_c$  leads to a rise in the values of the temperature  $T(y)$ , this is compatible with physical phenomena, but a reverse effect is noted for different values for the Reynolds number  $Re$ . Fig. 5 (b) elucidate the effect of the electric Rayleigh number  $L$  and the couple stress parameter  $S$  on the mean temperature  $T(y)$ , it is observed that the higher value of the Rayleigh number  $L$  leads to an increase in the mean temperature  $T(y)$ , but an opposite effects as the couple stress parameter  $S$  increases and for larges values of the Rayleigh number  $L$  and the couple stress parameter  $S$ , a very small variant occurs.

## VI. 2. The mean time-averaged electric potential

Fig. 6 (a,b) illustrates the nature of the mean time-averaged electric potential  $\varphi(y)$  for different values of the problem parameters. Fig. 6 (a) shows that the greater values of the Rayleigh number  $L$  and the Eckert number  $E_c$  increase the mean time-averaged electric potential near the region of the lower wall but reduce it in the region near the upper wall. From Fig. 6 (b), we have observed that the increasing of the



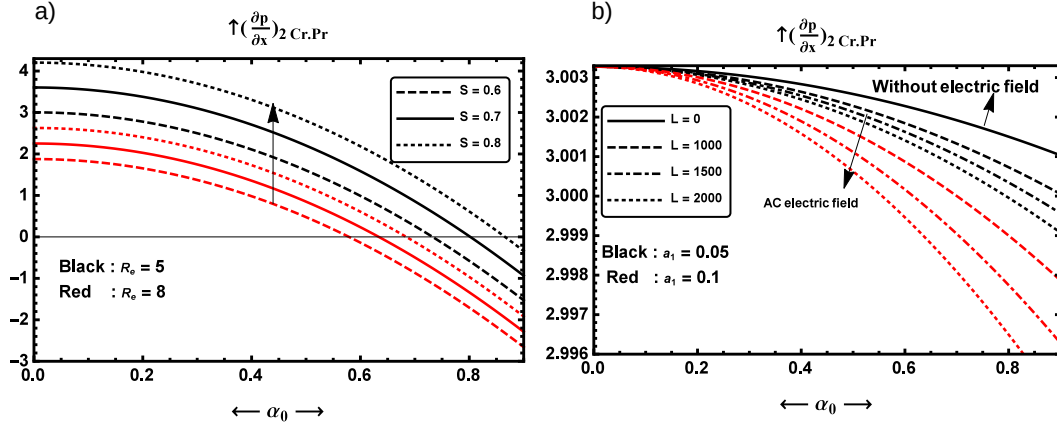


Fig. 7. Variation of the critical reflux op pressure vs  $\alpha_0$  for  $L_2 = 0.1$  and  $a_1 = 0.5$ ,  $a_0 = 0.4$ ,  $\frac{\partial p_2}{\partial x} = 10$ ,  $\alpha_0 = 0.5$  and  
 (a) different values of couple stress parameter  $S$  and Reynolds number  $R_e$  for  $L = 10000$ ,  $a_1 = 0.5$ .  
 (b) different values of electrical parameter  $a_1$  and Rayleigh number  $L$  for  $R_e = 5$ ,  $S = 0.8$

couple stress parameter  $S$  and Reynolds number  $Re$  produce an increase in the mean time-averaged electric potential  $\varphi(y)$  near the upper wall and an opposite behavior near the lower wall. As expected from Fig. 6 (a,b), the boundary conditions  $\varphi(y)$  (equ.20) are satisfied at the walls.

### VI. 3. Critical pressure gradient for reflux

The study of the critical pressure gradient for reflux is very important because the bacteria and some other materials sometimes move from the bladder to the kidney or from one kidney to the other in the direction opposite to the direction of urine flow. This phenomenon is referred to as "ureteral reflux" by physiologists following [26]. The riskiness of diseases such as tuberculosis, interstitial cystitis and duct stone are treated due to this reflux following [26]. Fig. 7 depicts the critical pressure gradient  $(\frac{\partial p}{\partial x})_{2Cr.Pr}$  which is plotted against the wave number  $\alpha_0$  in the range [0- 0.9]. From the behavior of Fig. 7, we observe that the relation between the critical pressure gradient  $(\frac{\partial p}{\partial x})_{2Cr.Pr}$  and wave number  $\alpha_0$  is inverse, i.e. the increase of the wave number reduces the critical pressure values. Fig. 7 (a) shows the effect of the Reynolds number  $R_e$  and the couple stress parameter  $S$  on the critical pressure gradient  $(\frac{\partial p}{\partial x})_{2Cr.Pr}$ . It is found that the increase of the Reynolds number  $R_e$  reduces the critical pressure gradient and an opposite effect with the increase of couple stress  $S$ . The effect of the electrical parameter and the electric Rayleigh number on the critical pressure gradient is shown in Fig. 7 (b), it can be conjectured that the increase of the electric Rayleigh number and electrical parameter increase values of the critical pressure gradient.

## VII. CONCLUSION

A numerical study for the peristaltic flow of a couple stress dielectric fluid (as special case of non-Newtonian) with

heat transfer and a vertical alternative current AC in a symmetric flexible sinusoidal wavy channel have been obtained. A parametric NDSolve package is used to solve a system of coupled non-linear partial differential equations. Graphs of mean average velocity, temperature and electric potential are drawn for various values of the couple stress parameter  $S$ , the pressure gradient  $\frac{\partial p_2}{\partial x}$ , electric Rayleigh number  $L$ , electric parameter  $a_1$ , Eckert number  $E_c$  and the Reynolds number  $R_e$ . The main findings can be summarized as follows:

- AC electric field accelerates the blood flow velocity and that leads to enhanced blood circulation, which is useful to eliminate the metabolic waste products and endogenous pains producing.
- In the absence of the couple stress parameter (Newtonian fluid), the electrical parameter  $a_1$  and electric Rayleigh number  $L$  have an increasing effect on the mean velocity in the region near the upper wall of the channel while it decreases in the region near to the lower one.
- when  $S \neq 0$ . The average velocity is higher in the presence of an alternative current AC electric field.
- the reflux phenomena of the fluid are less common for a fluid with a potential difference than that without a potential difference.
- The second order pressure gradient  $\frac{\partial p_2}{\partial x}$  has a significant influence on the reflux mean velocity.
- The couple stress parameter has a decreasing effect on the mean velocity.
- Mean average temperature increases as the Eckert number and the electric Rayleigh number  $L$  increase but a reverse effect for the Reynolds number and the couple stress parameter.
- The greater of the Eckert number and the electric Rayleigh parameter increase the mean time-averaged electric potential in the region near the lower wall but reduces in the region near the upper one and a reverse

effect for the Reynolds number and the couple stress parameter.

## References

- [1] H.H. Woodson and J.R. Melcher, *Electromechanical Dynamics* (John Wiley and Sons, New York, 1968).
- [2] M. Takashima, *The Stability of a Rotating Layer of the Maxwell Liquid Heated from Below*, Journal of the Physical Society of Japan **29**, 1061–1068 (1970).
- [3] M. Takashima and A.K. Ghosh, *Electrohydrodynamic Instability of Viscoelastic Liquid Layer*, Journal of the Physical Society of Japan **47** 1717–1722 (1979).
- [4] M.F. El-Sayed, M.H. Harouna, and D.R. Mostapha, *Electroconvection peristaltic flow of viscous dielectric liquid sheet in asymmetrical flexible channel*, Atomization and Sprays **25** 985-1011 (2015).
- [5] M.M. Bhatti, A. Zeeshan, R. Ellahi and N. Ijaz, *Heat and mass transfer of two-phase flow with Electric double layer effects induced due to peristaltic propulsion in the presence of transverse magnetic field*, Journal of Molecular Liquids (2017), doi:10.1016/j.molliq.2017.01.033.
- [6] N.S. Akbar, S. Nadeem, *Thermal and velocity slip effects on the peristaltic flow a six constant Jeffrey's fluid model*, International Journal of Heat Mass Transfer **55**, 3964–3970 (2012).
- [7] M. M. Bhatti, A. Zeeshan, R. Ellahi, *Heat transfer analysis on peristaltically induced motion of particle-fluid suspension with variable viscosity: clot blood model*, Computer Methods and Programs in Biomedicine (2016)
- [8] S. Hina, T. Hayat, S. Asghar and A. A. Hendi, *Influence of compliant walls on peristaltic motion with heat/mass transfer and chemical reaction*, International Journal of Heat and Mass Transfer **55**, pp.3386-3394 (2012).
- [9] Kh. S. Mekheimer, N. Saleem and T. Hayat, *Simultaneous effects of induced magnetic field and heat and mass transfer on the peristaltic motion of second-order fluid in a channel*, International Journal for Numerical Methods in Fluids, **70** 342–358 (2012).
- [10] T. Hayat, S. Noreen, M. Alhothuali, S. Asghar and A. Al-homaidan, "Peristaltic flow under the effects of an induced magnetic field and heat and mass transfer", International Journal of Heat and Mass Transfer, vol 55, , pp.443-452 (2002).
- [11] V. K. Stokes, Couple stresses in fluids. Physics of Fluids, vol. 9, pp. 1709-1715 (1966).
- [12] Kh. S. Mekheimer, Peristaltic transport of blood in a uniform and non-uniform channel, Applied mathematics and Computation, 153, (2004),763-777.
- [13] M. M. Bhatti, R. Ellahi and A. Zeeshan, Study of variable magnetic field on the peristaltic flow of Jeffrey fluid in a non-uniform rectangular duct having compliant walls, Journal of Molecular Liquids, 222 (2016) 101-108.
- [14] R. Ellahi, M. M. Bhatti and I. Pop, Effects of hall and ion slip on MHD peristaltic flow of Jeffrey fluid in a non-uniform rectangular duct, International Journal of Numerical Methods for Heat and Fluid Flow, 26 (2017) 1802-1820.
- [15] A.A. Khan, H. Usman, K. Vafai, R. Ellahi, *Study of peristaltic flow of magnetohydrodynamic Walter's B fluid with slip and heat transfer*, Scientia Iranica B **23**, 2650–2662 (2016).
- [16] M.M. Bhatti, A. Zeeshan, R. Ellahi, *Simultaneous effects of coagulation and variable magnetic field on peristaltically induced motion of Jeffrey nanofluid containing gyrotactic microorganism*, Microvascular Research **110**, 32–42 (2017).
- [17] Kh.S. Mekheimer, A.M. Salem, A.Z. Zaher, *Peristaltically induced flow due to a surface acoustic wavy wall*, Chinese Journal of Physics **51**, 954–968 (2013).
- [18] Kh. S. Mekheimer, A.M. Salem , A.Z. Zaher, *Peristaltically induced MHD slip flow in a porous medium due to a surface acoustic wavy wall*, Journal of the Egyptian Mathematical Society **22**, 143–151 (2014).
- [19] Y. Abd elmaboud, Kh.S. Mekheimer, A.I. Abdellateef, *Thermo properties of couple-stress fluid in an asymmetric channel with peristalsis*, Journal of Heat Transfer **135** (2013).
- [20] A.M. Abdulhadi, A.W. Saleh, *Effects of Couple Stress and Porous Medium on Transient Magneto Peristaltic Flow under the Action of Heat Transfer*, IOSR Journal of Mathematics, **12**, 71–83 (2016).
- [21] S. Akram, Kh. S. Mekheimer and S. Nadeem, *Influence of Lateral Walls on Peristaltic Flow of a Couple Stress Fluid in a Non-Uniform Rectangular Duct*, Appl. Math. Inf. Sci. **8**, 1127–1133 (2014).
- [22] R. Ellahi, M.M. Bhatti, C. Fetecau, K. Vafai, *Peristaltic Flow of Couple Stress Fluid in a Non-Uniform Rectangular Duct Having Compliant Walls*, Commun. Theor. Phys. **65**, 66–72 (2016).
- [23] S. Hina, M. Mustafa, T. Hayat and A. Alsaedi, Peristaltic flow of couple-stress fluid with heat and mass transfer: An application in biomedicine, Journal of Mechanics in Medicine and Biology **15**, 1–17 (2015).
- [24] K. Ramesh and M. Devakar, *Effects of heat and mass transfer on the peristaltic transport of MHD couple stress fluid through porous medium in a vertical asymmetric channel*, Journal of Fluids, 1–19 (2015).
- [25] A. Govindarajan ,E. P. Siva and M. Vidhya, Combined effect of heat and mass transfer on MHD Peristaltic transport of a couple stress fluid in a inclined asymmetric channel through a porous medium, International Journal of Pure and Applied Mathematics, 105 (2015) 685-707.
- [26] Y.C. Fung, C.S. Yih, *Peristaltic Transport*, J. Appl. Mech. **35**, 669–675 (1968).
- [27] K.H. Wolfgangand, A.M. Phillips, *Classical Electricity and Magnetism* (Addison-Wesley, 1955).



**Kh.S. Mekheimer** is Professor of Mathematics at Al-Azhar University, Faculty of Science, Mathematics Department, Naser City 11884, Cairo, EGYPT. He received BSc in 1984 at Faculty of Science, Ain-Shams University, MSc in 1990 and PhD in 1994 at Department of Mathematics, Faculty of Science, Al-Azhar University. From 1997 to 2003 he had worked as an assistant professor at Department of mathematics, King Abdu Al-Aziz University branch, Madinahh Munawwara, Saudi Arabia. From 2003 to now, he works a Professor of Applied Mathematics at Department of Mathematics, Al- Azhar University, Cairo, Egypt. His research fields interests are in the Branches of applied mathematics (physiological flow). He has published more than 100 research articles in international journals.



**W.M. Hassona** is a faculty member in the department of mathematics, faculty of science, Zagazig University. He received the BS in 1983, MSc degree in 1988, PhD in 1994 and assistant professor in 2015 In Mathematics from Faculty of Science, Zagazig University. His interest research area simulates the numerical and analytical treatments related the nonlinear deterministic and stochastic system.



**A.A. El-Shehhipy** received the BSc in 2003 at the Department of Mathematics in Faculty of Science, Minia University, El-Minia, Egypt. Furthermore, he received MS degree in Mathematics in 2009 and PhD in Mathematics in 2013 from Faculty of Science, Minia University. His interest research area simulates the numerical and analytical treatments related the nonlinear deterministic and stochastic system.



**A.Z. Zaher** is assistant lecturer in Engineering Mathematics and Physics Department, Faculty of Engineering - Shubra - Benha University. He received BSc in 2007 from Faculty of Science, Benha University and MSc in 2014 from faculty of science, Zagazig University. His research fields interests are in the Branches of applied mathematics (physiological flow).